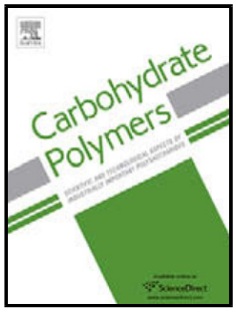

Title: Gums induced microstructure stability in Ca(II)-alginate beads containing lactase analyzed by SAXS

Authors: Maria Victoria Traffano-Schiffo, Marta Castro-Giraldez, Pedro J. Fito, Mercedes Perullini, Patricio R. Santagapita

PII: S0144-8617(17)31138-4
DOI: https://doi.org/10.1016/j.carbpol.2017.09.096
Reference: CARP 12841

To appear in:

Received date: 6-6-2017
Revised date: 26-9-2017
Accepted date: 28-9-2017

Please cite this article as: Traffano-Schiffo, Maria Victoria., Castro-Giraldez, Marta., Fito, Pedro J., Perullini, Mercedes., & Santagapita, Patricio R., Gums induced microstructure stability in Ca(II)-alginate beads containing lactase analyzed by SAXS.*Carbohydrate Polymers* https://doi.org/10.1016/j.carbpol.2017.09.096

Gums induced microstructure stability in Ca(II)-alginate beads containing lactase analyzed by SAXS

Maria Victoria Traffano-Schiffo[a], Marta Castro-Giraldez[a], Pedro J. Fito[a], Mercedes Perullini[b,c,*], Patricio R. Santagapita[d,e,*]

[a]Instituto Universitario de Ingeniería de Alimentos para el Desarrollo, Universidad Politécnica de Valencia, Camino de Vera s/n, 46022 Valencia, Spain.

[b]Universidad de Buenos Aires. Facultad de Ciencias Exactas y Naturales. Departamento de Química Inorgánica, Analítica y Química Física. C1428AOE, Buenos Aires, Argentina.

[c]CONICET-Universidad de Buenos Aires. Instituto de Química Física de los Materiales, Medio Ambiente y Energía (INQUIMAE). C1428AOE, Buenos Aires, Argentina.

[d]Universidad de Buenos Aires. Facultad de Ciencias Exactas y Naturales. Departamentos de Industrias y Química Orgánica. C1428AOE, Buenos Aires, Argentina.

[e]CONICET-Universidad de Buenos Aires. Instituto de Tecnología de Alimentos y Procesos Químicos (ITAPROQ). C1428AOE, Buenos Aires, Argentina.

*Corresponding authors: prs@di.fcen.uba.ar; mercedesp@qi.fcen.uba.ar

Highlights

- Structure at different scales of Ca(II)-alginate beads were assessed by SAXS
- Gums as second excipients induce a stabilization in the microstructure at rod scale
- Gums stabilize the size and density of the dimers and the interconnection of rods
- Guar gum improves the lactase activity during operation conditions

ABSTRACT

Previous works show that the addition of trehalose and gums in β-galactosidase (lactase) Ca(II)-alginate encapsulation systems improved its intrinsic stability against freezing and dehydration processes in the pristine state. However, there is no available information on the evolution in microstructure due to the constraints imposed by the operational conditions. The aim of this research is to study the time course of microstructural changes of Ca(II)-alginate matrices driven by the presence of trehalose, arabic and guar gums as excipients and to discuss how these changes influence the diffusional transport (assessed by LF-NMR) and the enzymatic activity of the encapsulated lactase.

The structural modifications at different scales were assessed by SAXS. The incorporation of gums as second excipients induces a significant stabilization in the microstructure not only at the rod scale, but also in the characteristic size and density of alginate dimers (basic units of construction of rods) and the degree of interconnection of rods at a larger scale, improving the performance in terms of lactase activity.

Keywords: alginate beads; hydrocolloids; encapsulation; β-galactosidase; microstructure; Small-Angle X-ray scattering (SAXS).

1. Introduction

In recent years, the encapsulation of β-galactosidase (lactase) in order to control its release and improve its stability against thermal and mechanical effects has been widely investigated (Traffano-Schiffo, Castro-Giraldez, Fito, & Santagapita, 2017b; Zhang, Zhang, Chen, McClements, & 2016; Zhang, Zhang, & McClements, 2017; Estevinho, Damas, Martins, & Rocha, 2014).

Alginate is one of the most used anionic polyelectrolytes for the encapsulation of bioactive compounds (Santagapita, Mazzobre, & Buera, 2012). It consists of (1→4)-linked residues of β-D-mannuronate (M) and α-L-guluronate (G), and in solution it generates a hydrogel matrix through the complexation of G-blocks with di- or trivalent cations such as Ca^{2+}, Mn^{2+}, Zn^{2+}, Al^{3+}, Cr^{3+}, and Ce^{3+} (Santagapita, Mazzobre, & Buera, 2011), embodying them into the cavities formed by a cooperative pairing of contiguous G-blocks (Stokke et al., 2000) forming the structure commonly known as "egg-box" (He, Liu, Li, & Li, 2016). Additionally, the sodium alginate solution can be gelled at acidic pH. Once a critical fraction of carboxylate residues are protonated, the decrease in the polymer charge density allows for chain-chain interactions leading to gelation. The inherent pH for the consolidation of H–alginate hydrogel is around 3.5, depending on the mannuronic (pK_a = 3.38) to guluronic acid (pK_a = 3.65) relative content of the employed alginate. Moreover, the Ca(II)–alginate structure can be obtained by cation exchange from a parent H–alginate hydrogel (Sonego, Santagapita, Perullini, & Jobbágy, 2016),

indicating a higher affinity of alginate polymer for Ca^{2+}. It has been demonstrated that the combined use of alginate with sugars and/or other biopolymers such as arabic and guar gums allows to improve the stability of enzymes within the hydrogel (Traffano-Schiffo et al., 2017b).

The alginate microstructure depends on several factors such as the alginate's concentration, average molecular weight and monomer composition (M/G ratio), as well as the presence of secondary excipients and the synthesis conditions (mainly the Ca^{2+} concentration and pH). On the other hand, the alginate bead constitutes an intrinsically inhomogeneous system, determined by the dropping method followed in conventional synthesis procedures. This method generates a Ca^{2+} gradient established from the surface to the core of the forming bead (Thu et al., 2000). All these parameters are related to the capacity of the hydrogel network to interact with the encapsulated biomolecule and the surrounding medium (Santagapita et al., 2011; Gombotz & Wee, 2012). Cross-linking and gelation of alginate was widely used for immobilization of bio-entities, from macromolecules to metazoans (Santagapita et al., 2011; Perullini et al., 2016). Beyond its high biocompatibility, by selection of the type of alginate and synthesis conditions, the pore size, degradation rate, and ultimately release kinetics can be finely controlled, allowing the design of controlled release systems (Tønnesen & Karlsen, 2002). Proteins immobilized in alginate matrices are released by two mechanisms: (i) diffusion of the protein through the pores of the polymer network and (ii) degradation of the polymer network. Analysis of Ca(II)-alginate gels by electron microscopies has shown that a very broad range of pore sizes (from 5 nm to 300 nm in diameter) can be obtained (Andresen et al., 1977; Agulhon et al., 2012). In a different approach, the porosity evaluated from size-

exclusion chromatography, smaller cut-off values in the order of 8-16 nm were obtained (Klein et al., 1983; Stewart & Swaisgood, 1993). It is worth noting that in the latter approach a relatively high compactness of the biopolymer network is expected from the synthesis conditions employed (homogeneous method and long-term aging in the crosslinking cation solution). Regardless of the initial pore size, the leakage of immobilized species in bare alginate matrices is well documented, not only for macromolecules but even for much higher species as whole-cells (Perullini et al., 2005; Zhang et al., 2016).

One of the most precise and powerful techniques to evaluate the microstructure of hydrogels is the small-angle X-ray scattering (SAXS). The SAXS method is able to reveal subtle differences in electron density within hydrogels cross-linked networks in the range 1-100 nm, providing information on the supramolecular structure formed by biopolymers (Waters et al., 2010). SAXS patterns are indicative of rod like objects formed as the accumulation of cross-linked alginate chain dimers randomly orientated, establishing junction zones of different multiplicity (Agulhon, Robitzer, David, & Quignard, 2012). Previous works of lactase encapsulation in Ca(II)-alginate beads (Traffano-Schiffo et al., 2017b; Traffano-Schiffo, Aguirre Calvo, Castro-Giraldez, Fito, & Santagapita, 2017a) revealed that the remaining lactase activity after storage, freezing and freeze/thaw cycles, and dehydration, preserved by trehalose, was even improved by the presence of gums. The microstructure of the beads generated at pH 3.8 showed rods with smaller cross-sectional radius and with lower compactness when gums were used as additives. However, there is no available information on the evolution of the microstructure due to the constraints imposed by the operational conditions. On the other hand, information regarding the

structure of the polymer chain dimers by analyzing SAXS curves at values of q higher than 1.5 nm^{-1} is presented for the first time. These "egg-box" structures were traditionally regarded as invariant blocks of construction of rods, and rods' structural changes were evaluated in terms of the multiplicity of the junction zones (i.e. the number of alginate dimers in the cross-section of the rod) (Stokke et al., 2000). Thus, the aim of this research is to study the time course of microstructural changes of Ca(II)-alginate matrices driven by the presence of trehalose, arabic and guar gums as excipients and to discuss how these changes influence the diffusional transport (assessed by LF-NMR) and the enzymatic activity of the encapsulated lactase in operation conditions.

2. Materials and Methods

2.1.Materials

The employed materials are listed below: sodium alginate (Algogel 5540) from Cargill S.A. (San Isidro, Buenos Aires, Argentina), molecular weight of $1.97 \cdot 10^5$ g/mol and mannuronate/guluronate ratio of 0.6; D-trehalosedihydrate (Hayashibara Co., Ltd., Shimoishii, Okayama, Japan/Cargill Inc., Minneapolis, Minnesota, USA), molecular weight of 378 g/mol; guar gum (Cordis S.A., Villa Luzuriaga, Buenos Aires, Argentina), molecular weight of 220.000 g/mol and a mannose/galactose ratio of 1.8; arabic gum (Biopack, Zárate, Buenos Aires, Argentina), molecular weight of 250.000 g/mol and a purity of 99%; β-galactosidase (lactase) from *Aspergillus Oryzae* (8.0 U/mg) (Sigma-Aldrich Co., Ltd., Saint Louis, USA). One enzymatic unit was defined as the amount of enzyme able to hydrolyze 1.0 μmol of lactose per minute at pH 4.5 at 30ºC.

2.2.Gel Beads Preparation and Characterization

Four different formulations for the encapsulation of the enzyme (E) were prepared, with the following composition: alginate (EA); alginate-trehalose (EAT); alginate-trehalose-guar gum (EATGG); alginate-trehalose-arabic gum (EATAG). All the solutions were prepared in 0.1 M acetate buffer pH 3.8. The final concentration of lactase was 0.775 mg/mL (slightly increased respect to Santagapita & Buera (2008) in order to give good activity values with a relative small quantity of beads (9) for this encapsulation system). The enzyme and the precursor solutions were carefully mixed and maintained at 4 ± 1 ºC in order to avoid enzyme activity losses. Taking into account that the isoelectric point of the enzyme is 4.61 (Dashevsky, 1998) and the pK_a values of alginate are 3.38 and 3.65 (Smidsrød, Larsen, Painter, & Haug, 1969), the buffer acetate at pH 3.8 was used in order to generate favorable electrostatic interactions between the negatively charged alginate and the positively charged enzyme. A peristaltic pump was used to drop 10 mL of the alginate-enzyme mixture into 100 mL of the gelling solution, according to the drop method described by Austin, Bower and Muldoon with some modifications (Austin, Bower, & Muldoon, 1996). For EA beads preparation, 1% (w/v) alginate solution containing lactase was dropped into 2.5% (w/v) $CaCl_2$ solution prepared in 0.1 M acetate buffer pH 3.8. For EAT, EATGG, and EATAG preparation, a 1% (w/v) alginate with 20% (w/v) trehalose with or without 0.25% (w/v) of guar or arabic gums containing the enzyme was dropped into the 2.5% (w/v) $CaCl_2$ solution supplemented with 20% (w/v) trehalose using the same procedure previously described.

The $CaCl_2$ solution (with or without trehalose) was maintained in a cold bath with constant stirring. A needle with 0.25 mm diameter and 6 mm length (Novofine 32 G, Novo Nordisk A/S, Bagsvaerd, Denmark) was used for the dropping. The pump speed was 9.0 ± 0 rpm. The distance between the needle and the $CaCl_2$ solution was 6.0 cm. After beads generation, they were maintained for 15 min in $CaCl_2$ solution (with constant stirring), and then they were washed 5 times with bidistilled cold water (5±1 °C) in order to remove free Ca^{2+}. Previous to SAXS measurements, beads were maintained at (5±1 °C) for 96 h. Control beads without enzyme were also prepared using the same methodology.

The beads were characterized in terms of size and shape by measuring the Feret's diameter and circularity by optical microscopy and a digital image processing technique, as previously reported (Traffano-Schiffo et al., 2017a), in order to ensure that the subset of 9 beads used for each experiment was representative of the total population.

2.3.Microstructure Analyses

Beads synthesized at pH 3.8 were incubated in 0.1 M acetate buffer pH 4.5 for different times (5, 10, 15, 20, 40, and 60 min). The microstructure characterization was performed by SAXS at the LNLS SAXS2 beamline in Campinas, Brazil, working at λ =0.1488 nm. The wave vector range was selected in the range 0.096 $nm^{-1} < q < 2.856\ nm^{-1}$. All the Ca(II)-alginate beads analyzed showed isotropic scattering and were modeled as a fractal system composed of rodlike structures, although the rigorous interpretation of experimental results as indicating "fractality" requires many orders of magnitude of power-law scaling (Sonego et al., 2016). Five

parameters were analyzed: i) α_1, the fractal dimension at distances higher than the characteristic size of the rods composing the structure (R_1), which describes the multiplicity of the junction zone, at $q < 0.28$ nm^{-1}; ii) α_2, the fractal dimension at distances lower than R_1, at $q > 0.55$ nm^{-1}, describing the degree of compactness within the rods; iii) R_1, the cross-sectional radius of the rods, which is given by $R_1 = R_g\sqrt{2}$, R_g being the mean gyration radius in the cross-section of the rods, which is obtained from the maximum exhibit by the Kratky plot at $q \approx 1/R_g$; iv) α_3, related to the connectivity between associated polymer chains forming dimers (basic units composing the rods) at $q > 1.5$ nm^{-1} and v) R_2, related to the outer radius of these aforementioned units.

The Kratky plot: scattering intensity multiplied by the square modulus of the scattering vector, $I(q)\cdot q^2$, as a function of the modulus of the scattering vector, q, gives a maximum value at the intersection of the α_1 and α_2 power law regions and a minimum value at the intersection of the α_2 and α_3 power law regions, allowing the calculation of parameters R_1 and R_2, respectively. All measurements were made in triplicate. Parameters α_1, α_2 and α_3 were evaluated from the slope of the scattering intensity averaged along azimuthal angles versus the scattering vector q in the log–log scale.

2.4.β-Galactosidase Activity

The enzyme activity was evaluated based on the absorbance values at 420 nm by using a Jasco V-630 UV-vis spectrophotometer (JASCO Inc., Maryland, USA) at room temperature and following the method described by Park, Santi, and Pastore, with some modifications (Park, Santi, & Pastore, 1979).

Each analysis was performed using a pool of 9 beads which were mixed with 0.25 mL of 0.25% (w/v) o-nitrophenyl-β-D-galactopyranoside (ONPG) (Sigma Chemical Co.) prepared with 0.1 M acetate buffer pH 4.5. Samples were incubated during 5, 10, 15, 20, 40, and 60 min at 33 ºC, without continuous stirring in order to avoid possible enzymatic activity losses, but gently shacked every 5 min to prevent diffusional limitations. The reaction was stopped adding 0.5 mL of sodium carbonate 10% (w/v) and 0.25 mL of sodium citrate 10% (w/v) was added to dissolve the beads and finally, 1.75 mL of distilled water was added for subsequent measurement of o-nitrophenol (ONP) at 420 nm. Measurements were made in triplicate.

The [ONP] accumulation was followed over time (5, 10, 15, 20, 40, or 60 min) in each of the studied systems (EA, EAT, EATAG or EATGG), as well as for a sample of free enzyme provided as a reference. The free enzyme system was prepared by using the same enzyme concentration employed for bead synthesis, using 30 µl aliquots for incubation instead of 9 beads, following the same procedure previously described. [ONP] values were normalized by the initial enzymatic activity after beads generation, since the initial amount of active enzyme present in each system is expected to be different as reported by Traffano-Schiffo et al. (2017a). The initial enzyme activity after bead generation was determined as described by Traffano-Schiffo et al. (2017a). Briefly, 9 beads were dissolved in 0.25 mL of 0.1 M citrate buffer pH 4.5 during 2 h at 4 ºC and without stirring in order to avoid enzymatic activity losses. Subsequently, 0.25 mL of 0.25 % (w/v) ONPG was added and incubated during 15 min at 33 ºC. Finally, the reaction was stopped adding 0.5 mL of sodium carbonate 10% (w/v) and 1.75 mL of distilled water for subsequent measurement of ONP at 420 nm.

The loading efficiency of the enzyme in the beads after generation was determined as previously described (Traffano-Schiffo et al., 2017a), obtaining similar results to those reported in literature for the same enzyme (Sen, Nath, Bhattacharjee, Chowdhury, & Bhattacharya, 2014) in the range 88-92%.

2.5.Low Field Nuclear Magnetic Resonance (LF-NMR)

Diffusion coefficient of water (D_w) was measured by time resolved low field proton nuclear magnetic resonance (^{1}H-LF-NMR) in a Bruker Minispec mq20 (Bruker Biospin Gmbh, Rheinstetten, Germany) with a 0.47 T magnetic field operating at a resonance frequency of 20 MHz. Two samples of each bead system were previously equilibrated at 25.00 ± 0.01 °C in a thermal bath (Haake, model Phoenix II C35P, Thermo Electron Corporation Gmbh, Karlsruhe, Germany).

Measurements were performed through the pulsed magnetic field gradient-spin echo sequence (Stejskal, & Tanner, 1965). The applied magnetic field gradient intensity was calibrated in the range between 1.4 and 2.4 T/m by employing 1.25 g/L $CuSO_4 \cdot 5H_2O$ water solution, characterized by a known D_w value ($2.3 \cdot 10^{-9}$ m^2/s at 25 ºC) (Hester-Reilly, & Shapley, 2007). The bead samples were analyzed by setting the magnetic field gradient amplitude to 1.4 T/m, t (the time between 90 and 180 pulses) to 7.5 ms, δ to 0.5 ms, and Δ to 7.5 ms. The number of scans, the recycle delay and gain were 16, 2 s and 69 dB, respectively. D_w was calculated following the procedure reported by Santagapita et al. (2013).

2.6.Statistical Analyses

The statistical analyses were performed by one-way ANOVA with Tukey`s post test by using Prism 6 (GraphPad Software Inc., San Diego, CA, USA) in order to determine significant differences between the mean values of beads of different compositions on the measured parameters.

3. Results and Discussion

Figure 1 shows the scattering intensity as a function of the scattering vector for a representative sample of Ca(II)-alginate hydrogel containing lactase (EA), incubated in 0.1 M acetate buffer pH 4.5 for 20 minutes. A schematic representation of the scale of different structural parameters derived from SAXS scattering experiments is included. SAXS scattering curves can be divided in three regions: at low, intermediate and high q values. From the slope of the log-log plot at low q, α_1 parameter is indicative of the interconnectivity of the rods composing the alginate network. At intermediate q values, α_2 parameter represents the compactness within the rods, and at high q values α_3 parameter characterizes the connectivity between associated polymer chains forming dimers. Besides, two characteristic radii of gyration can be derived: R_1, the cross-sectional radius of the rods, and R_2 denoting the size of the polymer dimers basic units. Kratky plots ($q^2 \cdot I(q)$ vs q) were used to evaluate R_1 as already reported (Sonego et al., 2016; Thu et al., 2000; Gombotz & Wee, 2012; Waters et al., 2010; Agulhon et al., 2012). Characteristic SAXS profiles and Kratky plots from all the systems analyzed are presented in Supplementary File (Figures S1 and S2, respectively).

Control systems without the enzyme were also conducted in order to analyze the influence of the presence of lactase in the microstructure of the alginate gel. Except for subtle changes, the microstructure remains the same for all the systems under study and thus it can be concluded that the enzyme is not directly involved in the formation of the alginate rods. A complete description of these results is included in Supplementary File (Figure S3).

Figure 2 shows the evolution of the microstructure parameters related to the size and compactness of the rods (R_1 and α_2, respectively). For the non-incubated beads (synthesized at pH 3.8), the addition of trehalose with or without gums affected the extent of the rod formation, reducing the radius of the rods (Figure 2a, time = 0) as well as their compactness (Figure 2b, time = 0), as previously discussed Traffano-Schiffo et al. (2017a).

As a general trend, the increase in pH (from 3.8 to 4.5) generates a decrease both in size and compactness of the rods for the systems in the absence of gums. However, the presence of guar or arabic gums generates a much stable structure, maintaining a constant rod size and significantly reducing the initial drop in α_2, as well as further changes along incubation time. It is worth noting that the synthesis pH is close to the pK_a of guluronic acid and thus the contribution of H-alginate to the consolidation of the alginate network cannot be neglected. Therefore, at low free Ca^{2+} concentrations, an increase in pH would lead to an increase in alginate polymer repulsion with a concomitant reduction of the compactness due to the loss of the H-alginate contribution to the structure. This can also explain the reduction in the rod size, considering that some of the alginate chains can be released from the junction zones.

The presence of gums seems to reduce alginate-alginate repulsion which suggests that they are located in within the rods, particularly between associated polymer chains forming dimers. Thus, the relatively high values of α_2 during operation conditions for EATGG and EATAG samples show that the presence of gums induces a high packing of these alginate dimers within the rods. This hypothesis was deeply analyzed by considering the evolution of α_3 and R_2, the nanostructure parameters describing the size and compactness of these dimers, basic units of construction of the rods (as shown in Figure 3 a and b, respectively). The presence of gums modulates the nanostructure of the dimers generating an increase in their size and a decrease in their compactness, compatible with the hypothesis of gums being intercalated within the dimers. Furthermore, the addition of gums once again induced a higher stability toward an increase in pH. However and regardless of the presence of different excipients, the nanostructure of dimers shows similar characteristics and remains stable during the operation conditions at pH 4.5.

In order to go a step further in the analysis of the microstructure of the hydrogels during the operation conditions, the evolution of α_1 parameter for each bead composition was analyzed (Figure 4). The parameter α_1 is related to the degree of interconnection of the rods composing the structure. Values of α_1 around 1 correspond to randomly oriented rods, while a α_1 value close to 2 is indicative of a network composed of well interconnected rods (Sonego et al., 2016). All the systems under study showed initial values of α_1 around 1.5 (i. e. for the hydrogel obtained at

pH 3.8), characteristic of a consolidated network. The formulations lacking gums additives showed an increase in α_1 when exposed to the operation pH 4.5, reaching values of around 1.8 (for the system with trehalose, EAT, after 20 minutes of incubation). Once established the degree of interconnectivity of rods in aged systems, the α_1 parameter is expected to remain constant in time. One plausible explanation for α_1 fluctuations relies on the increased availability of alginate polymer chains resulting from the partial dissolution of rods, as previously discussed regarding parameter α_3 and R_2. Thus, the presence of free alginate chains could induce the formation of new connections in the network, establishing a new equilibrium. In line with this, the presence of gums induces stabilization in the microstructure, resulting in no significant variations in α_1 parameter both with the initial increase in pH and throughout the operation time at pH 4.5.

Water self-diffusion coefficient (D_w) determined by LF-NMR for Ca(II)-alginate beads gives valuable information of the overall decrease on the mobility of protons (especially those from water), modulated by the exchange between them and the protons of the biopolymers (Sonego et al., 2016; Aguirre Calvo, Busch, & Santagapita, 2017). The magnitude of this decrease depends on reduced flexibility of the biopolymer chains with respect to water and the aggregation state. As expected, all alginate systems gelled at pH 3.8 showed reduced D_w values in comparison with water, $(2.30 \pm 0.01) \times 10^{-9}$ m^2 s^{-1} (Holz, Heil, & Sacco, 2000), as shown in Table 1. The presence of trehalose in the hydrogels further reduced D_w values. However, the concomitant addition of gums induced a slight increase of D_w with respect to the EAT system. These changes are in well agreement with the water activity and

content previously reported (Traffano-Schiffo et al., 2017a). Besides, the measure of D_w can give an idea of the water transport through the aqueous pores, which can be also related with the diffusion of other water soluble species. The dramatic drop in D_w can be explained from the evolution of parameters α_2 and R_1, which show a significantly higher size and compactness of the rods for the hydrogel in the absence of additives (EA). This is consistent with highly packed rods which in turn enclose more alginate dimers, reducing the tortuosity through the aqueous pores.

[a-c] E, enzyme; A, alginate; T, trehalose; AG, arabic gum; GG, guar gum. Standard deviation values are included. Different letters on the columns indicate significant differences between means ($p < 0.05$).

Then, bearing in mind that the modulation of the enzyme activity will be given by the entrance of substrate through the pores as well as by the overall microstructure of the Ca(II)-alginate gel, the addition of excipients would be expected to modulate lactase activity. Figure 5 shows the effect of the composition of the beads on the performance of β-galactosidase during operating conditions by measuring the accumulation of ONP concentration (colored compound) spectrophotometrically.

As expected, all beads systems showed a reduced [ONP] accumulation with respect to the free enzyme system. It can be observed that the EAT shows the lowest ratio of enzymatic activity; however, the addition of gums as second excipients reverts this detriment caused by trehalose, increasing for guar gum containing beads (EATGG) β-galactosidase activity above the standards of bear Ca(II)-alginate hydrogel (EA).

EAT beads present the worst possible scenario: low diffusion and poor microstructure stability. The incorporation of gums palliates this by improving the intrinsic transport properties of the initial hydrogel, in one hand, and more importantly by stabilizing its microstructure. The latter seems to be a determining factor in the performance of these systems during operating conditions.

4. Conclusions

Though being a key in preserving enzymatic activity toward freezing and dehydration processes, the addition of trehalose as additive in Ca(II)-alginate lactase encapsulation systems prompts important structural changes leading to a loss of enzymatic activity during operation conditions. Trehalose drastically reduces the water self-diffusion coefficient in the starting hydrogel system (synthesized at pH 3.8), concomitant with the reduction in size and compactness of the structure at the scale of alginate rods. The incorporation of gums as second excipients does not revert this last effect, nevertheless induces a significant stabilization in the microstructure not only at the rod scale, but also at smaller and bigger scales. On one hand, gums are shown to induce an important modulation in the characteristic size and density of alginate dimers (basic units of construction of rods). On the other hand and highly related to this, the variation in the degree of interconnection of rods evidenced in EA and EAT systems (i.e. in the absence of gums) is impeded. It is worth noting that in EA and EAT, this process is facilitated by free alginate polymer chains that become available from partial rod dissolution. Thus, this microstructure stabilization induced by the concomitant addition of guar gum results in an increased

lactase activity during operation conditions, improving the performance of the systems with trehalose even above the bear Ca(II)-alginate matrix.

Acknowledgements

This work was supported by the Brazilian Synchrotron Light Laboratory (LNLS, Brazil, proposal SAXS1-20160278), Universidad de Buenos Aires (UBACyT 20020130100610BA), Agencia Nacional de Promoción Científica y Tecnológica (ANPCyT PICT 2013 0434 and 2013 1331), CIN-CONICET (PDTS 2015 n° 196), and Consejo Nacional de Investigaciones Científicas y Técnicas. The author María Victoria Traffano-Schiffo wants to thank "Programa para la Formación de Personal Investigador (FPI)" Pre-doctoral Program of the Universitat Politècnica de València (UPV) for support her PhD studies and also her mobility to Argentina.

Appendix A. Supplementary data

Figure S1. log–log SAXS profile plots of representative of Ca(II)-alginate lactase beads for the different systems, incubated in 0.1 M acetate buffer pH 4.5 at different times. E, enzyme; A, alginate; T, trehalose; AG, arabic gum; GG, guar gum. Figure S2. Kratky plots of SAXS data obtained for Ca(II)-alginate beads containing enzyme for the four systems analyzed. The curves at each incubation time were arbitrary shifted up. E, enzyme; A, alginate; T, trehalose; AG, arabic gum; GG, guar gum. Figure S3. Parameter α_1 (a) and α_2 (b) of the microstructure derived from log-log SAXS profiles and R_1 (cross-sectional radius of the rods) (c), deduced from the maxima obtained on Kratky plots. Standard deviations values are included. Different

letters on the columns (a-e) indicate significant differences between values with $p<$ 0.05. E, enzyme; A, alginate; T, trehalose; AG, arabic gum; GG, guar gum.

References

Agulhon, P., Robitzer, M., David, L., & Quignard, F. (2012). Structural regime identification in ionotropic alginate gels: influence of the cation nature and alginate structure. *Biomacromolecules,* 13(1), 215-220.

Andresen, I. L.; Skipnes, O.; Smidsrød, O.; Ostgaard, K. & Hemmer, P. C. (1977). Some biological functions of matrix components in benthic algae in relation to their chemistry and the composition of seawater. *ACS Symposium Series,* 48, 361-381.

Austin, L., Bower, J. J., & Muldoon, C. (1996). The controlled release of leukaemia inhibitory factor (LIF) from gels. In *Proceeding of the International Symposium on Controlled Release of Bioactive Materials,* 23, 739-740.

Calvo, T. R. A., Busch, V. M., & Santagapita, P. R. (2017). Stability and release of an encapsulated solvent-free lycopene extract in alginate-based beads. *LWT-Food Science and Technology,* 77, 406-412.

Dashevsky, A. (1998). Protein loss by the microencapsulation of an enzyme (lactase) in alginate beads. *International Journal of Pharmaceutics*, 161(1), 1-5.

Estevinho, B. N., Damas, A. M., Martins, P., & Rocha, F. (2014). Microencapsulation of β-galactosidase with different biopolymers by a spray-drying process. *Food Research International*, 64, 134-140.

Gombotz, W. R., & Wee, S. F. (2012). Protein release from alginate matrices. *Advanced Drug Delivery Reviews*, 64, 194-205.

He, X., Liu, Y., Li, H., & Li, H. (2016). Single-stranded structure of alginate and its conformation evolvement after an interaction with calcium ions as revealed by electron microscopy. *RSC Advances*, 6(115), 114779-114782.

Hester-Reilly, H. J., & Shapley, N. C. (2007). Imaging contrast effects in alginate microbeads containing trapped emulsion droplets. *Journal of Magnetic Resonance*, 188(1), 168-175.

Holz, M., Heil, S. R., & Sacco, A. (2000). Temperature-dependent self-diffusion coefficients of water and six selected molecular liquids for calibration in accurate ^{1}H NMR PFG measurements. *Physical Chemistry Chemical Physics*, 2(20), 4740-4742.

Klein, J., Stock, J. & Vorlop, K. -D. (1983). Pore Size and Properties of Spherical Ca-Alginate Biocatalysts. *European Journal of Applied Microbiology Biotechnology*, 18, 86-91.

Park, Y. K., Santi, M. S. S., & Pastore, G. M. (1979). Production and characterization of β-galactosidase from *Aspergillus oryzae*. *Journal of Food Science*, 44(1), 100-103.

Perullini, M., Jobbágy, M., Soler-Illia, G. J. A. A., Bilmes, S. A. (2005). Cell growth at cavities created inside silica monoliths synthesized by sol-gel. *Chemistry of Materials*, 17(15), 3806-3808.

Perullini, M., Orias, F., Durrieu, C., Jobbágy, M. & Bilmes, S. A. (2014) Co-encapsulation of *Daphnia magna* and microalgae in silica matrices, a stepping stone toward a portable microcosm. *Biotechnology Reports*, 4, 147-150.

Santagapita, P. R., & Buera, M. P. (2008). Trehalose–water–salt interactions related to the stability of β-galactosidase in supercooled media. *Food Biophysics*, 3(1), 87-93.

Santagapita, P. R., Mazzobre, M. F., & Buera, M. P. (2011). Formulation and drying of alginate beads for controlled release and stabilization of invertase. *Biomacromolecules*, 12(9), 3147-3155.

Santagapita, P. R., Mazzobre, M. F., & del Pilar Buera, M. (2012). Invertase stability in alginate beads: Effect of trehalose and chitosan inclusion and of drying methods. *Food Research International*, 47(2), 321-330.

Santagapita, P., Laghi, L., Panarese, V., Tylewicz, U., Rocculi, P., & Dalla Rosa, M. (2013). Modification of transverse NMR relaxation times and water diffusion coefficients of kiwifruit pericarp tissue subjected to osmotic dehydration. *Food and Bioprocess Technology*, 6(6), 1434-1443.

Sen, P., Nath, A., Bhattacharjee, C., Chowdhury, R., & Bhattacharya, P. (2014). Process engineering studies of free and micro-encapsulated β-galactosidase in batch and packed bed bioreactors for production of galactooligosaccharides. *Biochemical Engineering Journal*, 90, 59-72.

Smidsrød, O., Larsen, B., Painter, T., & Haug, A. (1969). The role of intramolecular autocatalysis in the acid hydrolysis of polysaccharides containing 1,4-linked hexuronic acid. *Acta Chemica Scandinavica*, 23(5), 1573-1580.

Sonego, J. M., Santagapita, P. R., Perullini, M., & Jobbágy, M. (2016). Ca (II) and Ce (III) homogeneous alginate hydrogels from the parent alginic acid precursor: a structural study. *Dalton Transactions*, 45(24), 10050-10057.

Stejskal, E. O., & Tanner, J. E. (1965). Spin diffusion measurements: spin echoes in the presence of a time-dependent field gradient. *The Journal of Chemical Physics*, 42(1), 288-292.

Stewart, W. W. & Swaisgood, H. E. (1993). Characterization of calcium alginate pore diameter by size-exclusion chromatography using protein standards. *Enzyme Microbiology Technology*, 15, 922-927.

Stokke, B. T., Draget, K. I., Smidsrød, O., Yuguchi, Y., Urakawa, H., & Kajiwara, K. (2000). Small-angle x-ray scattering and rheological characterization of alginate gels. 1. Ca− alginate gels. *Macromolecules*, 33(5), 1853-1863.

Thu, B., Gåserød, O., Paus, D., Mikkelsen, A., Skjåk-Bræk, G., Toffanin, R., Vittur, F. & Rizzo, R. (2000). Inhomogeneous alginate gel spheres: An assessment of the polymer gradients by synchrotron radiation-induced x-ray emission, magnetic resonance microimaging, and mathematical modeling. *Biopolymers*, 53(1), 60-71.

Tønnesen, H. H. & Karlsen, J. (2002) Alginate in Drug Delivery Systems. *Journal of Drug Development and Industrial Pharmacy*, 28 (6), 621-630.

Traffano-Schiffo, M. V., Aguirre Calvo, T. R., Castro-Giraldez, M., Fito, P. J., & Santagapita, P. R. (2017a). Alginate beads containing lactase: stability and microstructure. *Biomacromolecules*, 18, 1785-1792.

Traffano-Schiffo, M. V., Castro-Giraldez, M., Fito, P. J., & Santagapita, P. R. (2017b). Encapsulation of lactase in Ca(II)-alginate beads: effect stabilizers and drying methods. *Food Research International*, *in press.*

Waters, D. J., Engberg, K., Parke-Houben, R., Hartmann, L., Ta, C. N., Toney, M. F., & Frank, C. W. (2010). Morphology of photopolymerized end-linked poly (ethylene glycol) hydrogels by small-angle X-ray scattering. *Macromolecules*, 43(16), 6861-6870.

Zhang, B. -B., Wang, L., Charles, V., Rooke, J. C., & Su, B. -L. (2016). Robust and Biocompatible Hybrid Matrix with Controllable Permeability for Microalgae Encapsulation. *ACS Applied Materials and Interfaces*, 8(14), 8939-8946.

Zhang, Z., Zhang, R., & McClements, D. J. (2017). Lactase (β-galactosidase) encapsulation in hydrogel beads with controlled internal pH microenvironments: Impact of bead characteristics on enzyme activity. *Food Hydrocolloids*. 67, 85-93.

Zhang, Z., Zhang, R., Chen, L., & McClements, D. J. (2016). Encapsulation of lactase (β-galactosidase) into κ-carrageenan-based hydrogel beads: Impact of environmental conditions on enzyme activity. *Food Chemistry*, 200, 69-75.

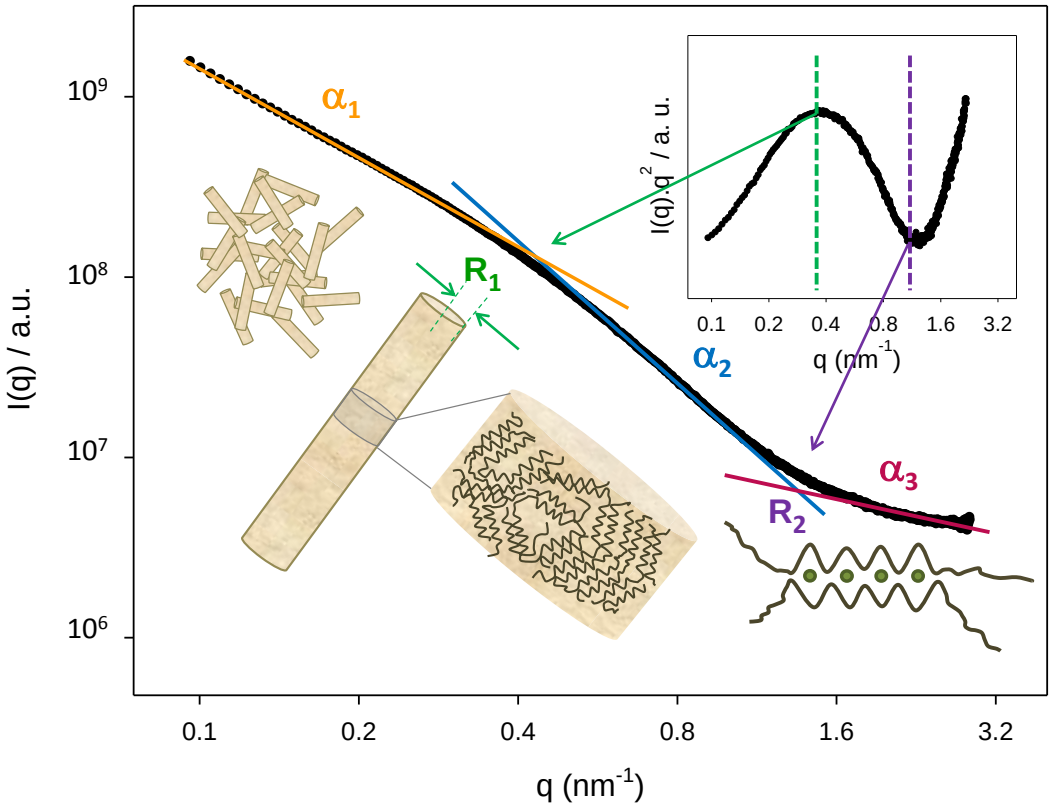

Figure 1. log–log SAXS profile plot of a representative sample of Ca(II)-alginate hydrogel containing lactase (EA), incubated in 0.1 M acetate buffer pH 4.5 for 20 minutes. Parameters α_1, α_2 and α_3 were evaluated from the slope of the scattering intensity at low, intermediate and high q values, respectively. The cross-sectional radius of the rods (parameter R_1) and the characteristic size of the Ca(II)-alginate dimers (parameter R_2) was obtained from the Kratky plot (inset).

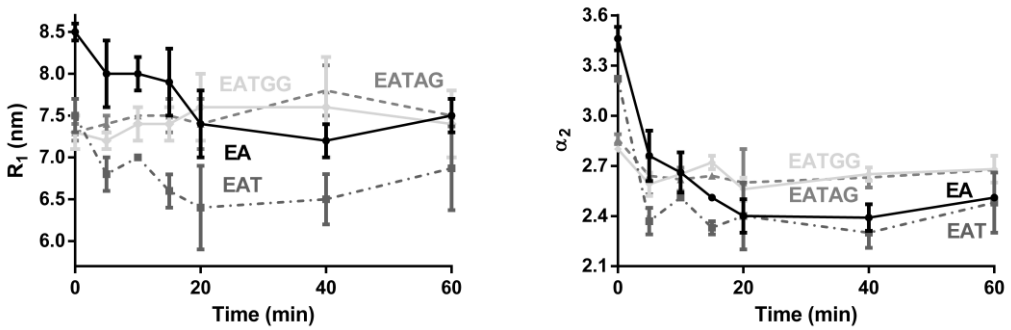

Figure 2. Microstructure parameters of Ca(II)-alginate beads synthesized at pH 3.8 vs. time of incubation in 0.1 M acetate buffer pH 4.5. a. Rod cross-sectional radius (R_1) deduced from the maxima obtained on Kratky plots. b. Fractal dimension at distances lower than R_1 or parameter α_2 of the microstructure derived from log-log SAXS profiles. Standard deviations values are included. E, enzyme; A, alginate; T, trehalose; AG, arabic gum; GG, guar gum.

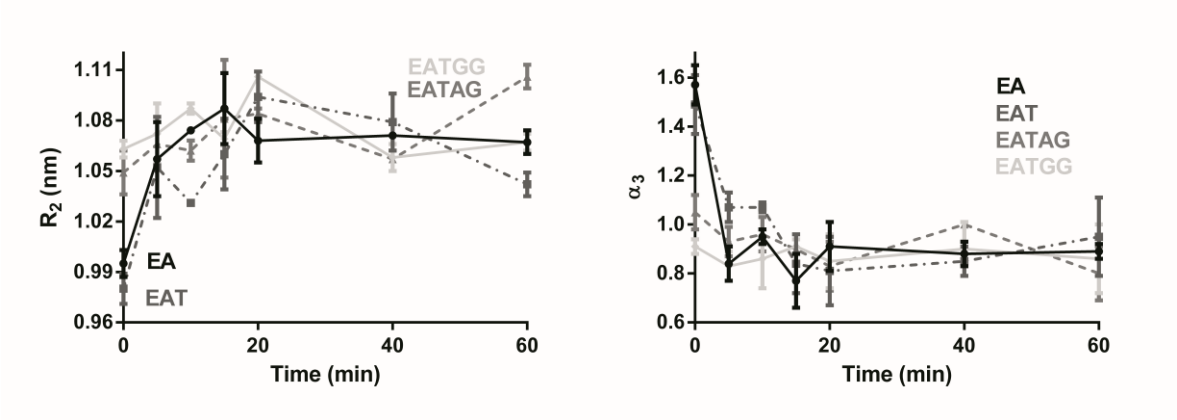

Figure 3. Microstructure parameters of Ca(II)-alginate beads synthesized at pH 3.8 vs. time of incubation in 0.1 M acetate buffer pH 4.5. a. Characteristic size of the Ca(II)-alginate dimers (R_2) deduced from the minima obtained on Kratky plots. b. Fractal dimension at distances lower than R_2 or parameter α_3 of the microstructure derived from log-log SAXS profiles. Standard deviations values are included. E, enzyme; A, alginate; T, trehalose; AG, arabic gum; GG, guar gum.

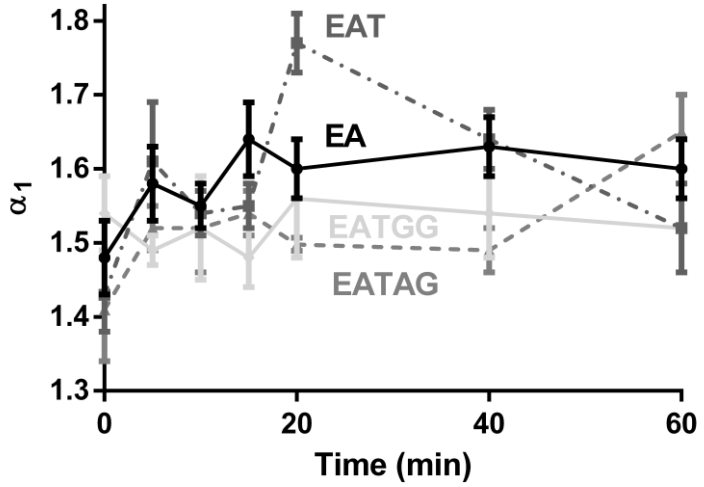

Figure 4. Fractal dimension at distances higher than R or parameter α_1 of the microstructure derived from log-log SAXS profiles. Standard deviation values are included. E, enzyme; A, alginate; T, trehalose; AG, arabic gum; GG, guar gum.

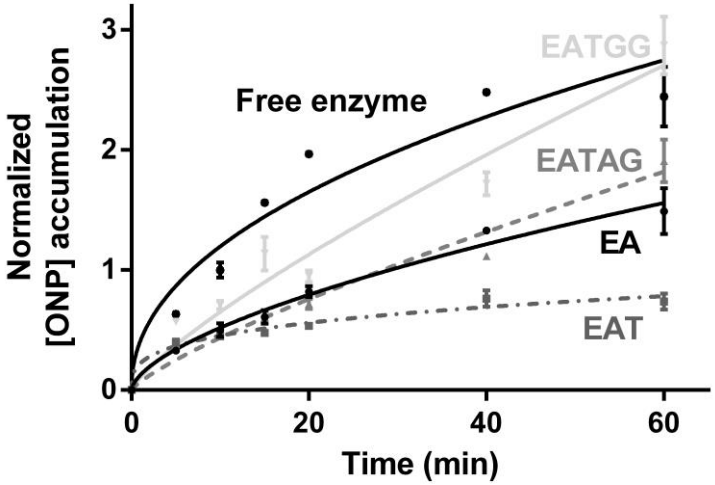

Figure 5. Normalized [ONP] accumulation in beads *vs.* time of incubation in 0.1 M acetate buffer pH 4.5. A control system (free enzyme) was included for comparison. The absolute concentration of ONP after 15 minutes of incubation is $4.0 \cdot 10^{-5}$ M for the control system. Standard deviations values are included. E, enzyme; A, alginate; T, trehalose; AG, arabic gum; GG, guar gum.

Table 1. Diffusion coefficients of water (D_w) in beads containing lactase determined by LF-NMR at 25 °C.

System	**D_w (10^{-9} m^2/s)**
EA	2.1 ± 0.03[a]
EAT	1.492 ± 0.011[c]
EATAG	1.6 ± 0.02[b]
EATGG	1.613 ± 0.013[b]